

Formulation And Evaluation Of Olorofim Containing Antifungal Nanogel

Dr. Kiran D. Baviskar, Mr. Nilesh Ramesh Patil , Dr. Bharat Vijaykumar Jain, Dr. Sandip Pawar, Dr. Tanvir Shaikh

Department of Pharmaceutics

Smt. Sharadchandrika Suresh Patil College of Pharmacy, Chopda, Maharashtra, India.

Olorofim, an antifungal compound from the orotomide class, acts by inhibiting dihydroorotate dehydrogenase (DHODH), a crucial enzyme involved in pyrimidine biosynthesis. This inhibition disrupts DNA synthesis, cellular growth, and division, making orlorofim an effective treatment for invasive fungal infections, including those resistant to traditional antifungal agents.

Developing and accessing a nanogel formulation containing orlorofim may provide enhanced therapeutic benefits against filamentous fungi, especially azole-resistant strains. Nanogels are particularly advantageous due to their ability to load high quantities of drugs and offer controlled drug release, potentially improving the antifungal efficacy of orlorofim.

Keywords: Nanogel, Antifungal, Olorofim, Fourier Transform Infrared Spectroscopy.

INTRODUCTION: The term "Nanogel" was first introduced to describe cross-linked, multifunctional networks composed of poly-ions and non-ionic polymers, initially designed for delivering polynucleotides. Nanogels consist of nanosized particles created through physical or chemical crosslinking of polymer networks, which swell in appropriate solvents, as described by Du et al. (2010). These systems have demonstrated their capability to deliver drugs in a controlled, consistent, and targeted manner. With advancements in polymer science, it is now feasible to develop smart nanosystems suitable for treatment, diagnostics, and clinical trials (Gota et al., 2009).

Nanogels are three-dimensional hydrogel structures within the nanoscale range, formed from crosslinked polymer networks that can absorb and retain large amounts of water without dissolving in aqueous environments. They can be synthesized using natural polymers, synthetic polymers, or combinations of both. Their specific properties—such as size, charge, porosity, amphiphilicity, softness, and degradability—can be tailored by modifying the chemical composition of the nanogels. Although often spherical, new synthetic techniques allow for the creation of nanogels in diverse shapes, including core-shell or core-shell-corona structures, where at least one layer is crosslinked for stability. Due to their hydrophilic nature, nanogels are highly biocompatible, offering a high loading capacity for various molecules. Their unique physical properties provide advantages over other nanomaterials in biomedical applications.

Nanogels serve as protective carriers, shielding loaded molecules from degradation and aiding the delivery process by leveraging characteristics such as stimuli responsiveness, softness, and swelling, which enable controlled, site-specific release. Their adaptable design supports the inclusion of diverse materials ranging from inorganic nanoparticles to biomacromolecules like proteins and DNA. This multifunctionality surpasses that of many other nanoparticulate systems, allowing nanogels to integrate components with varied physical properties without losing their gel-like behavior. Nanogels have emerged as

promising platforms for in vivo diagnostics and imaging, addressing the limitations of inorganic nanomaterials, such as instability, low solubility, and rapid elimination by the immune system. Nanohybrids—nanogels incorporated with inorganic materials—represent a new category of imaging agents, accommodating various diagnostic and imaging elements for medical applications. While they are yet to become part of routine clinical use, nanogels highlight significant potential in combination therapy and targeted drug delivery. Despite their broad application spectrum, hurdles remain that prevent nanogels from achieving widespread clinical adoption. Comprehensive reviews on nanogel synthesis and biomedical applications underscore both their potential and the challenges that need to be addressed for clinical advancement. These obstacles must be overcome to fully realize nanogels as versatile tools in modern medicine.

MATERIALS AND METHODS:

Preparation of Stock and Buffer Solutions:

1. **Hydrochloric Acid Buffer (pH 1.2):** Combine 50 mL of 0.2 M potassium chloride and 85 mL of 0.2 M HCl in a 200 mL volumetric flask, then dilute with water to reach the desired volume.
2. **Phosphate Buffer (pH 6.8):** Dissolve 60.5 g of disodium hydrogen phosphate and 46 g of potassium dihydrogen phosphate in water. Add 100 mL of 0.02 M disodium EDTA and 20 mg of mercuric chloride, then dilute with water to make up a total of 1000 mL.
3. **Phosphate Buffer (pH 7.4):** Mix 50 mL of 0.2 M potassium dihydrogen phosphate with 39.1 mL of 0.2 M sodium hydroxide in a 200 mL volumetric flask, and dilute with water to complete the volume.
4. **Sodium Hydroxide Solution (0.2 M):** Dissolve 8.0 g of sodium hydroxide in 1000 mL of distilled water.
5. **Potassium Dihydrogen Phosphate Solution (0.2 M):** Dissolve 27.218 g of potassium dihydrogen orthophosphate in 1000 mL of distilled water.
6. **Potassium Chloride Solution (0.2 M):** Dissolve 14.91 g of potassium chloride in 1000 mL of distilled water.

Preformulation Study:

Preformulation work forms the foundation for the development of a dosage form with a new or existing drug candidate. It involves determining the fundamental physical and chemical properties of the drug molecule and its derived properties, providing essential information for combining the drug with pharmaceutical excipients to create a dosage form. This initial learning phase is termed Preformulation.

Organoleptic Properties:

The drug sample of Olorofim was assessed for its organoleptic characteristics, including appearance, color, and odor.

Melting Point:

The melting point of Olorofim was determined using the open capillary method with a melting point apparatus. Measurements were performed in triplicate for accuracy.

Solubility:

The solubility of Olorofim was tested in various solvents, including water, acetonitrile, methanol, and ethanol.

Ultraviolet-Visible Spectroscopy:

a) Determination of Maximum Absorbance (λ_{max}):

The UV spectrum of Olorofim was obtained using a UV Shimadzu double-beam spectrophotometer. A 10 mg quantity of the drug was dissolved in methanol to prepare stock solutions (100 µg/ml) in acetonitrile. Spectra were recorded within the 200–400 nm wavelength range to determine the maximum absorbance (λ_{max}).

b) FTIR Spectroscopy:

The infrared spectrum of Olorofim was recorded using a Fourier Transform Infrared (FTIR) spectrophotometer (Model: FTIR, Bruker) at wave numbers ranging from 4000 to 50 cm^{-1} . The Attenuated Total Reflection (ATR) method was employed for analysis, enabling direct measurement of powder samples. This technique involves pressing the sample against a high-refractive-index prism and measuring the infrared spectrum through internally reflected infrared light.

Drug-Excipients Compatibility Study:

Drug-excipient compatibility was analyzed via liquid FTIR spectroscopy. Olorofim was mixed with excipients, such as oil, surfactant, and polymer, in equal proportions. The IR spectrum of the mixture was obtained using NaCl cells.

Formulation and Development of Nanogel:

Table 1: Composition of Nanogel formulation as per 3² full factorial designs

Formulation code	F1	F2	F3	F4	F5	F6	F7	F8	F9
Ingredients					%				
Olorofim (w/w)	0.1	0.1	0.1	0.1	0.1	0.1	0.1	0.1	0.1
Almond Oil (v/v)	0.3	0.3	0.3	0.2	0.2	0.2	0.1	0.1	0.1
Tween 80 (v/v)	0.525	0.525	0.525	0.525	0.525	0.525	0.525	0.525	0.525
Propylene glycol (v/v)	0.175	0.175	0.175	0.175	0.175	0.175	0.175	0.175	0.175
Methyl Paraben (w/w)	0.003	0.003	0.003	0.003	0.003	0.003	0.003	0.003	0.003
Propyl Paraben (w/w)	0.001	0.001	0.001	0.001	0.001	0.001	0.001	0.001	0.001

BHT	0.01	0.01	0.01	0.01	0.01	0.01	0.01	0.01	0.01
Water (v/v)	10	10	10	10	10	10	10	10	10

Formulation of Olorofim Nanogel:

Following the trial batches, excipients and their respective concentration ranges were finalized. The formulation chart was generated using Design Expert 12.0 software. This software was utilized to design and optimize Solid Lipid Nanoparticles (SLN) for Olorofim through a systematic approach.

The Design of Experiments (DOE) methodology offers a structured framework for making purposeful alterations to input factors in a process to examine their impact on output. DOE has found applications across diverse industries, including agriculture, pharmaceuticals, chemicals, electronics, automotive, and manufacturing sectors. Service industries have also leveraged DOE to gather process data and perform insightful analysis.

Preparation of gel:

Table 2: Composition of gel

Sr. No.	Ingredients (% w/w)	Quantity
1	Carbopol 934	0.1%
2	Triethanolamine	0.01%
3	Water (q.s.)	10

A measured amount of carbopol 934 was dispersed in distilled water at 40°C. Triethanolamine was then added to adjust the solution to the desired pH range. Continuous and uniform stirring was ensured throughout the process. The resulting gel formulation was stored in a refrigerator for 24 hours to stabilize.

Evaluation of Nanogel-Based Gel:

Determination of pH:

The pH of the formulation was analyzed using a digital pH meter. The electrode was thoroughly rinsed with distilled water, then immersed in the formulation to measure its pH.

Measurement of Viscosity:

The viscosity of the formulated nanogel was evaluated using a Brookfield Viscometer (RVDV-I Prime, Brookfield Engineering Laboratories, USA) equipped with spindle 63. The sample to be measured was transferred into a beaker and allowed to settle for 30 minutes at a controlled assay temperature of 25±1°C before the viscosity measurement.

Spreadability:

The spreadability of the gel formulations was determined using two glass slides of standard dimensions. A sample of the gel was placed on one slide, and another slide was placed on top, sandwiching the gel. The slides were pressed to remove any air bubbles, and excess gel was wiped off. The time taken for the upper slide to completely detach was noted. Spreadability was calculated using the formula:

$$S = M \cdot L/T$$

Where: **M** = weight tied to the upper slide **L** = length of the glass slides **T** = time taken to separate the slides.
spectrophotometer.

Accelerated Stability Studies of Gel:

Stability studies were carried out following established guidelines. The prepared gels were packed into aluminum collapsible tubes (5 g each) and subjected to stability testing under various conditions:

- 5°C
- 25°C/60% RH
- 30°C/65% RH
- 40°C/75% RH
- 60 ± 2°C

The tests were conducted over a period of three months, with samples withdrawn at 15-day intervals. The gels were evaluated for physical appearance, pH, rheological properties, and pharmaceutical content.

RESULTS AND DISCUSSION

Performulation study:

Organoleptic properties:

Table 3: Organoleptic properties of Olorofim

Drug	Properties	Observed Results
Olorofim	Appearance	Likely a crystalline or powder form in its raw state.
	Colour	often white or off-white
	Odour	Minimal or neutral, as it is a pharmaceutical compound.

Melting Point:

The melting point of compound was measured and reported as follows:

Table 4: Melting Point of Olorofim

Drug	Observed Value	Reported Value
Olorofim	155-156 ⁰ c	152-156 ⁰ c

Solubility

Solubility of Olorofim has been tabulated in the following table:

Table 5: Solubility of Olorofim

Solvent	Solubility
Water	Insoluble
Methanol	Soluble

Acetonitrile	Soluble
DMSO	Soluble
Ethanol	Soluble

Solubility and its solubility features was utilised for the UV spectroscopy and drug content.

Ultraviolet – Visible Spectroscopy study:

Determination of (λ_{\max}) of Olorofim in Methanol:



Fig. No.1: Ultraviolet Spectra of Olorofim in Methanol

Solubility determination of Olorofim:

Solubility determination of Olorofim in surfactants and co-surfactant

Table 6: Solubility of Olorofim in different surfactants and cosurfactant

Sr. No.	Excipients	Solubility (mg/ml)
1	Tween 20	28.03
2	Span 20	3.02
3	Tween 80	37.33
4	Span 80	30.41
5	Propylene glycol	35.66

Fourier Transform Infrared Spectroscopy

The FTIR spectrum of Olorofim has been shown in figure.

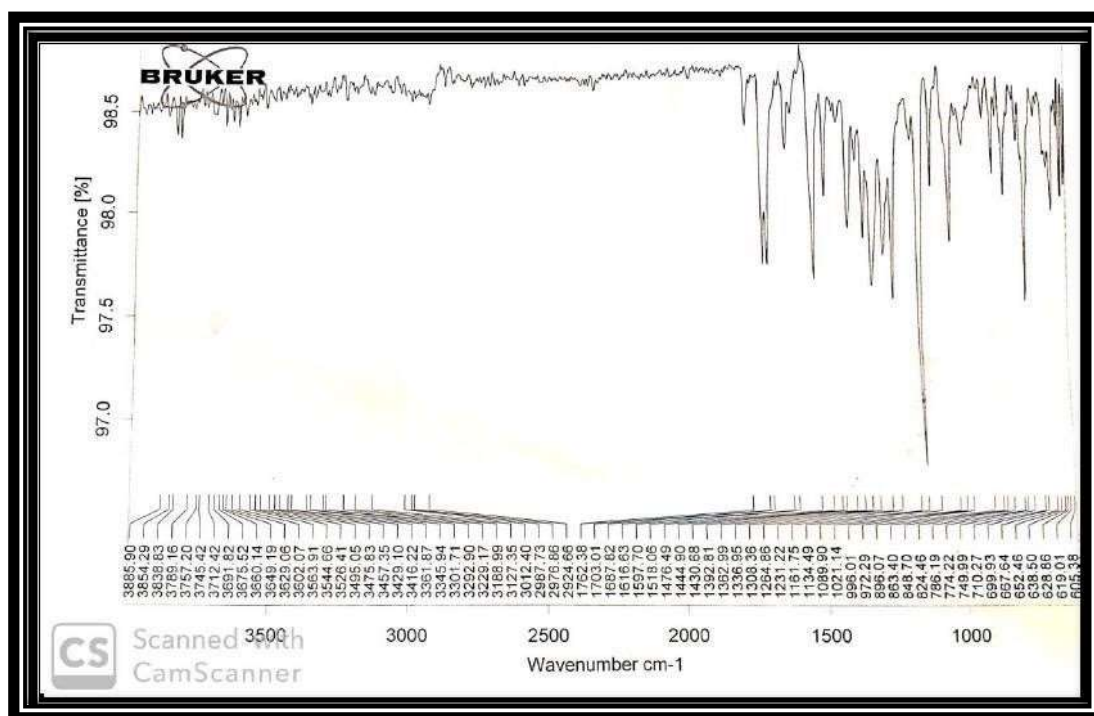


Fig. No. 2: Representative IR spectrum of Olorofim

Table 7: Functional groups present in I.R. of Olorofim

Sr. No.	Functional groups	Observed values (cm ⁻¹)	Standard values (cm ⁻¹)
1.	NH Stretch	3495.05	3500-3100
2.	C=O Stretch	1703.01	1725-1705
3.	C-O Stretch	1264.86	1300-1000
4.	C-H Bending	1444.90	1450-1375
5.	C=C	1616.63	1680-1600
6.	S=O	1362.99	1375-1300

The absorption bands observed in Olorofim are indicative of the functional groups within its molecular structure. These bands serve as confirmation of the identity and purity of the Olorofim sample utilized in the study.

Compatibility study

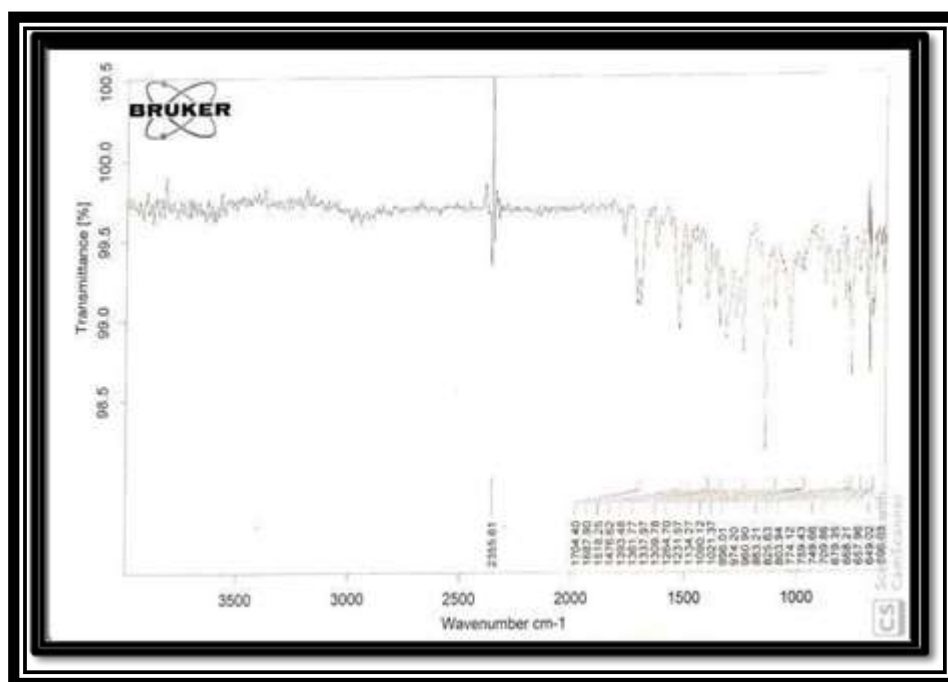


Fig. No.3: FTIR of Physical Mixture Table

Table 8: Interpretation of FTIR Spectrum of physical mixture

Functional Group	Pure drug	Physical mixture
NH Stretch	Yes	Yes
C=O Stretch	Yes	Yes
C-O Stretch	Yes	Yes
C-H Bending	Yes	Yes
C=C	Yes	Yes
S=O	Yes	Yes

Evaluation of Nanogel:**Physical appearance:**

Table 9: Physical appearance of formulations

Sr. No.	Parameters	Inference
1	Colour	Translucent gel
2	Homogeneity	Homogeneous
3	Consistency	Consistent

The physical appearance of the Nanogel formulation was found to be Translucent, homogeneous and consistent.

pH:

The pH values of various nanogel formulations, as presented in Table 10, were found to range between 6.31 and 6.84.

Table 10: pH values of formulation

Sr. No.	Formulation code	Observed pH (\pm SD)
1	F1	6.60 \pm 0.025
2	F2	6.75 \pm 0.018
3	F3	6.55 \pm 0.011
4	F4	6.45 \pm 0.011
5	F5	6.43 \pm 0.0158
6	F6	6.33 \pm 0.011
7	F7	6.31 \pm 0.005
8	F8	6.40 \pm 0.018
9	F9	6.53 \pm 0.026

Viscosity

The viscosity values of formulations are shown in the following table 11:

Table 11: Viscosity of formulations

Rpm	Viscosity (cP) at Room Temperature								
	Formulation Code								
	F1	F2	F3	F4	F5	F6	F7	F8	F9
10	14960	13450	14500	13750	12500	13500	14500	13500	12000
20	14200	12390	14000	13400	12250	12440	14250	12500	11709
30	13050	12050	13445	12350	11200	12203	13900	12000	10500
40	13000	11500	12230	12010	11000	11253	12750	11500	9850
50	12350	10420	11520	11250	10950	10504	12520	11200	9230

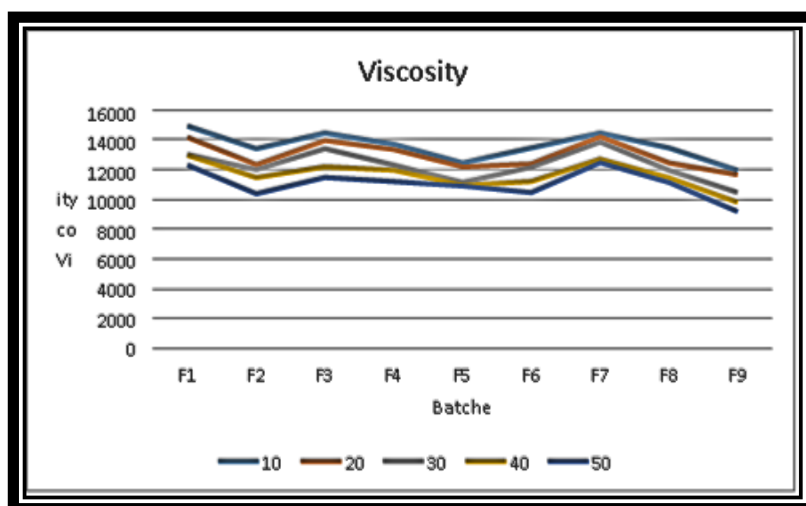


Fig. No. 4: Viscosity of formulation

Spreadability:

The spreadability of nanogels plays a crucial role in their effectiveness as topical formulations.

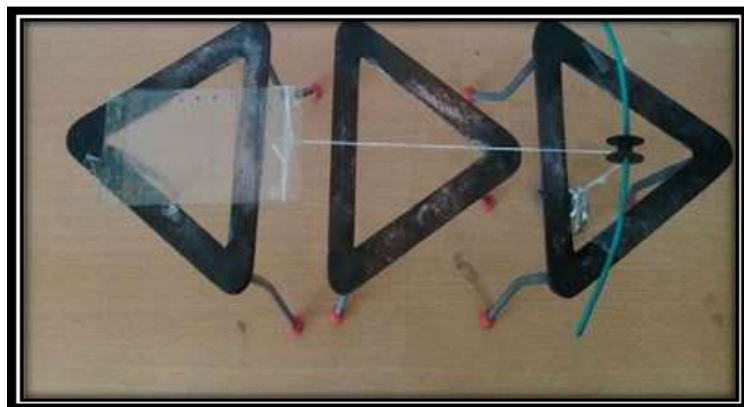


Fig. No. 5: Spreadability Apparatus

Table 12: Spreadability values of formulation

Sr. No.	Formulation code	Spreadability (g.cm/sec)± S.D.
1	F1	17.77 ± 0.025
2	F2	16 ± 0.035
3	F3	15.38 ± 0.028
4	F4	15.68 ± 0.018
5	F5	15.09 ± 0.032
6	F6	14.81 ± 0.012
7	F7	15.53 ± 0.012
8	F8	15.23 ± 0.011

9	F9	15.84 ±0.018
---	----	--------------

Drug Content

The drug content of formulation has shown in following table:

Table 13: Drug content of formulation

Sr. No.	Formulation code	Drug content (%)± SD
1	F1	96±0.5
2	F2	91.91±0.7
3	F3	95±0.7
4	F4	93.91±0.7
5	F5	94±0.7
6	F6	72±0.7
7	F7	68±1.09
8	F8	82±1.07
9	F9	64.91±1.43

Stability study:

Stability study of Optimized batch F1 was done at Room Temperature.

Table 14: Stability Study data for F1 formulation at Accelerated condition (40° C± 2° C, 75 % RH±5% RH)

Sr. No	Observations		Before Stability Testing	During study
				3 rd month
1	Clarity		Translucent	Translucent
2	pH		6.60±0.025	6.60±0.008
3	% Drug content		96±0.5	95.97± 0.5
4	Viscosity	10	12961cp	10233 cp
		20	11590cp	10123cp
		30	11821cp	9876cp
		40	10478cp	10122cp

CONCLUSION:

To enhance the delivery and efficacy of olorofim, a novel antifungal targeting dihydroorotate dehydrogenase (DHODH), through nanogel formulation The development and evaluation of an antifungal nanogel containing olorofim showcased its effectiveness as a delivery system for treating invasive fungal infections, especially those resistant to standard treatments. With optimized characteristics such as pH, viscosity, spreadability,

and drug content, the nanogel proved suitable for topical applications. Stability tests validated its durability under varying conditions, while swelling and drug release assessments demonstrated its ability to provide controlled and targeted medication delivery. Thus, the formulated nanogel represents a promising solution for improving the antifungal effectiveness of olorofim.

ACKNOWLEDGEMENT: The authors are thankful to the Principal, Smt. Sharadchandrika Suresh Patil College of Pharmacy, Chopda, Maharashtra, India. necessary facilities for research work.

CONFLICTS OF INTEREST: Authors have no conflicts of interest to declare.

REFERENCES:

1. Pfaller M.A., Pappas P.G., Wingard J.R. Invasive Fungal Pathogens: Current Epidemiological Trends. *Clin. Infect. Dis.* 2006;43:S3–S14. doi: 10.1086/504490.
2. Rauseo A.M., Coler-Reilly A., Larson L., Spec A. Hope on the Horizon: Novel Fungal Treatments in Development. *Open Forum Infect Dis.* 2020;7:ofaa016. doi: 10.1093/ofid/ofaa016.
3. Vallabhaneni S., Mody R.K., Walker T., Chiller T. The Global Burden of Fungal Diseases. *Infect Dis. Clin. N. Am.* 2016;30:1–11. doi: 10.1016/j.idc.2015.10.004.
4. Brown G.D., Denning D.W., Gow N.A., Levitz S.M., Netea M.G., White T.C. Hidden killers: Human fungal infections. *Sci. Transl. Med.* 2012;4:165rv13. doi: 10.1126/scitranslmed.3004404.
5. Kosmidis C., Denning D.W. The clinical spectrum of pulmonary aspergillosis. *Thorax.* 2015;70:270–277. doi: 10.1136/thoraxjnl-2014-206291.
6. Verweij P.E., Mellado E., Melchers W.J. Multiple-triazole-resistant aspergillosis. *N. Engl. J. Med.* 2007;356:1481–1483. doi: 10.1056/NEJMc061720.
7. Lestrade P.P.A., Meis J.F., Melchers W.J.G., Verweij P.E. Triazole resistance in *Aspergillus fumigatus*: Recent insights and challenges for patient management. *Clin. Microbiol. Infect.* 2019;25:799–806. doi: 10.1016/j.cmi.2018.11.027.
8. Enoch D.A., Yang H., Aliyu S.H., Micallef C. The Changing Epidemiology of Invasive Fungal Infections. *Methods Mol. Biol.* 2017;1508:17–65. doi: 10.1007/978-1-4939-6515-1_2.
9. Safdar A., Ma J., Saliba F., Dupont B., Wingard J.R., Hachem R.Y., Mattiuzzi G.N., Chandrasekar P.H., Kontoyiannis D.P., Rolston K.V., et al. Drug-induced nephrotoxicity caused by amphotericin B lipid complex and liposomal amphotericin B: A review and meta-analysis. *Medicine (Baltimore)* 2010;89:236–244. doi: 10.1097/MD.0b013e3181e9441b.
10. Townsend R., Dietz A., Hale C., Akhtar S., Kowalski D., Lademacher C., Lasseter K., Pearlman H., Rammelsberg D., Schmitt-Hoffman A., et al. Pharmacokinetic Evaluation of CYP3A4-Mediated Drug-Drug Interactions of Isavuconazole with Rifampin, Ketoconazole, Midazolam, and Ethinyl Estradiol/Norethindrone in Healthy Adults. *Clin. Pharmacol. Drug. Dev.* 2017;6:44–53.
11. Verweij P.E., Chowdhary A., Melchers W.J., Meis J.F. Azole Resistance in *Aspergillus fumigatus*: Can We Retain the Clinical Use of Mold-Active Antifungal Azoles? *Clin. Infect. Dis.* 2016;62:362–368. doi: 10.1093/cid/civ885.
12. Perlin D.S., Rautemaa-Richardson R., Alastruey-Izquierdo A. The global problem of antifungal resistance: Prevalence, mechanisms, and management. *Lancet Infect. Dis.* 2017;17:e383–e392.
13. Chowdhary A., Kathuria S., Xu J., Meis J.F. Emergence of azole-resistant *aspergillus fumigatus* strains due to agricultural azole use creates an increasing threat to human health. *PLoS Pathog.* 2013;9:e1003633. doi: 10.1371/annotation/4ffcf1da-b180-4149-834c-9c723c5dbf9b.
14. Resendiz Sharpe A., Lagrou K., Meis J.F., Chowdhary A., Lockhart S.R., Verweij P.E. Triazole resistance surveillance in *Aspergillus fumigatus*. *Med. Mycol.* 2018;56(Suppl. S1):83–92.
15. Hurst S.F., Berkow E.L., Stevenson K.L., Litvintseva A.P., Lockhart S.R. Isolation of azole-resistant *Aspergillus fumigatus* from the environment in the south-eastern USA. *J. Antimicrob. Chemother.* 2017;72:2443–2446.

16. Wiederhold N.P. Antifungal resistance: Current trends and future strategies to combat. *Infect. Drug Resist.* 2017;10:249–259.
17. Dannaoui E. Antifungal resistance in mucorales. *Int. J. Antimicrob. Agents.* 2017;50:617–621. doi: 10.1016/j.ijantimicag.2017.08.010.
18. Buil J.B., Rijs A.J.M.M., Meis J.F., Birch M., Law D., Melchers W.J.G., Verweij P.E. In vitro activity of the novel antifungal compound F901318 against difficult-to-treat *Aspergillus* isolates. *J. Antimicrob. Chemother.* 2017;72:2548–2552.
19. Oliver J.D., Sibley G.E.M., Beckmann N., Dobb K.S., Slater M.J., McEntee L., du Pré S., Livermore J., Bromley M.J., Wiederhold N.P., et al. F901318 represents a novel class of antifungal drug that inhibits dihydroorotate dehydrogenase. *Proc. Natl. Acad. Sci. USA.* 2016;113:12809–12814.
20. Jørgensen K.M., Astvad K.M.T., Hare R.K., Arendrup M.C. EUCAST Determination of Olorofim (F901318) Susceptibility of Mold Species, Method Validation, and MICs. *Antimicrob. Agents Chemother.* 2018;62:e00487-18.
21. Wiederhold N.P., Najvar L.K., Jaramillo R., Olivo M., Birch M., Law D., Rex J.H., Catano G., Patterson T.F. The Orotomide Olorofim Is Efficacious in an Experimental Model of Central Nervous System *Coccidioidomycosis*. *Antimicrob. Agents Chemother.* 2018;62:e00999-18.
22. du Pré S., Beckmann N., Almeida M.C., Sibley G.E.M., Law D., Brand A.C., Birch M., Read N.D., Oliver J.D. Effect of the Novel Antifungal Drug F901318 (Olorofim) on Growth and Viability of *Aspergillus fumigatus*. *Antimicrob. Agents Chemother.* 2018;62:e00231-18. doi: 10.1128/AAC.00231-18.
23. Rivero-Menendez O., Cuenca-Estrella M., Alastruey-Izquierdo A. In vitro activity of olorofim (F901318) against clinical isolates of cryptic species of *Aspergillus* by EUCAST and CLSI methodologies. *J. Antimicrob. Chemother.* 2019;74:1586–1590. doi: 10.1093/jac/dkz078.
24. Seyedmousavi S., Chang Y.C., Law D., Birch M., Rex J.H., Kwon-Chung K.J. Efficacy of Olorofim (F901318) against *Aspergillus fumigatus*, *A. nidulans*, and *A. tanneri* in Murine Models of Profound Neutropenia and Chronic Granulomatous Disease. *Antimicrob. Agents Chemother.* 2019;63:e00129-19. doi: 10.1128/AAC.00129-19.
25. Lim W., Eadie K., Konings M., Rijnders B., Fahal A.H., Oliver J.D., Birch M., Verbon A., van de Sande W. *Madurella mycetomatis*, the main causative agent of eumycetoma, is highly susceptible to olorofim. *J. Antimicrob. Chemother.* 2020;75:936–941. doi: 10.1093/jac/dkz529.